Frequent *IGF2/H19* Domain Epigenetic Alterations and Elevated *IGF2* Expression in Epithelial Ovarian Cancer

Susan K. Murphy,[1,2] Zhiqing Huang,[1] Yaqing Wen,[1] Monique A. Spillman,[1] Regina S. Whitaker,[1] Lauren R. Simel,[1] Teresa D. Nichols,[1] Jeffrey R. Marks,[2,3] and Andrew Berchuck[1,2]

[1]Division of Gynecologic Oncology, [2]Duke Institute for Genome Sciences and Policy, and [3]Department of Surgery, Duke University Medical Center, Durham, North Carolina

Abstract

Overexpression of the imprinted *insulin-like growth factor-II* (*IGF2*) is a prominent characteristic of gynecologic malignancies. The purpose of this study was to determine whether *IGF2* loss of imprinting (LOI), aberrant *H19* expression, and/or epigenetic deregulation of the *IGF2/H19* imprinted domain contributes to elevated *IGF2* expression in serous epithelial ovarian tumors. *IGF2* LOI was observed in 5 of 23 informative serous epithelial ovarian cancers, but this did not correlate with elevated expression of *IGF2 H19* RNA expression levels were also found not to correlate with *IGF2* transcript levels. However, we identified positive correlations between elevated *IGF2* expression and hypermethylation of CCCTC transcription factor binding sites 1 and 6 at the *H19* proximal imprint center (*P* = 0.05 and 0.02, respectively). Hypermethylation of CCCTC transcription factor sites 1 and 6 was observed more frequently in cancer DNA compared with lymphocyte DNA obtained from women without malignancy (*P* < 0.0001 for both sites 1 and 6). Ovarian cancers were also more likely to exhibit maternal allele-specific hypomethylation upstream of the imprinted *IGF2* promoters when compared with normal lymphocyte DNA (*P* = 0.004). This is the same region shown previously to be hypomethylated in colon cancers with *IGF2* LOI, but this was not associated with LOI in ovarian cancers. Elevated *IGF2* expression is a frequent event in serous ovarian cancer and this occurs in the absence of *IGF2* LOI. These data indicate that the epigenetic changes observed in these cancers at the imprint center may contribute to *IGF2* overexpression in a novel mechanistic manner.

(Mol Cancer Res 2006;4(4):283–92)

Introduction

Ovarian cancer is the leading cause of death from gynecologic malignancies because the majority of cases are not detected until the disease has metastasized. We previously did a microarray-based analysis on serous cancers from individuals with early-stage and advanced-stage disease (1). The gene expression profiles obtained from these cancers indicated that more than half exhibited a high level of expression of the *insulin-like growth factor-II* (*IGF2*) gene, which is located at chromosome 11p15.5. High *IGF2* expression was recently shown to be a predictor of poor prognosis in epithelial ovarian cancers and was associated with the most aggressive forms of this disease (2). In addition, serum levels of IGF2 are one of four combinatorial diagnostic markers used in a newly developed test for early detection of ovarian cancer (3). Despite the strong association between *IGF2* expression and ovarian malignancies, little is known about the molecular underpinnings of *IGF2* deregulation in this disease.

IGF2 encodes a potent mitogenic growth factor that is active in early development and plays an important role in embryonic and fetal growth (4). IGF2 binds to the IGF-I receptor to initiate intracellular signaling cascades that lead to cell proliferation (5, 6). Increased expression of *IGF2* is a common feature of both pediatric and adult malignancies (5), and mounting evidence implicates IGF2 as a major factor contributing to oncogenesis.

IGF2 transcription is subject to genomic imprinting, an epigenetic form of gene regulation that leads to mRNA production from only one allele in a manner depending on the sex of the parent from whom the allele was inherited. *IGF2* expression is from the paternal allele, whereas the maternal allele is normally inactive. *IGF2* imprinting is relaxed in many different types of tumors, including osteosarcoma (7), lung adenocarcinomas (8), head and neck squamous cell adenocarcinomas (9, 10), Wilms' tumor (11), prostate cancer (12), and colorectal carcinomas (13-17). This loss of imprinting (LOI) occurs when there is abnormal activation of the maternal copy of *IGF2* and the resultant overexpression contributes to tumor growth. *IGF2* expression is coordinately regulated with the maternally expressed *H19* gene that produces a noncoding RNA. Studies in mice and humans have shown that the reciprocal imprinting of these two genes is at least partially dependent on the presence of binding sites for the CCCTC transcription factor (CTCF; ref. 18), which are located upstream of the *H19* promoter and comprise part of the germ-line imprinting mark (19).

Received 8/17/05; revised 1/18/06; accepted 2/14/06.
Grant support: Ovarian Cancer Research Fund (S.K. Murphy) and Gail Parkins Ovarian Awareness Foundation.
The costs of publication of this article were defrayed in part by the payment of page charges. This article must therefore be hereby marked advertisement in accordance with 18 U.S.C. Section 1734 solely to indicate this fact.
Requests for reprints: Susan K. Murphy, Division of Gynecologic Oncology, Duke University Medical Center, Box 91012, Durham, NC 27708. Phone: 919-681-3423; Fax: 919-684-5336. E-mail: murph035@mc.duke.edu

doi:10.1158/1541-7786.MCR-05-0138

CTCF is a zinc finger transcription factor that functions to preclude potential associations between promoters and enhancers by inducing formation of chromatin structure that physically separates the relevant sequences (20, 21). CTCF is blocked from binding the *H19* proximal binding sites by methylation on the paternal chromosome. CTCF binds the unmethylated maternal chromosome and prevents enhancers located downstream of *H19* from accessing the maternal *IGF2* promoter. Acquisition of methylation on the maternal chromosome in this region or loss of methylation from the paternal chromosome occurs in a highly tumor-specific manner. For example, in bladder cancer, paternal hypomethylation leads to biallelic *H19* expression (22), whereas in Wilms' tumor, maternal hypermethylation and biallelic *IGF2* expression are common (11, 23-25).

H19 RNA itself has also been ascribed a role in the regulation of *IGF2*. Using a hepatoblastoma cell line disomic for chromosome 11, Wilkin et al. showed that transgenic expression of *H19* antisense transcripts resulted in increased *IGF2* mRNA and protein expression, whereas expression of *H19* sense transgenes resulted in *IGF2* transcript and protein levels equivalent to control cells (26). The level of *H19* RNAs in Wilms' tumor is also found to inversely correlate with levels of *IGF2* mRNA (27). In this study, *H19* RNAs were found in polysomes, indicative of *H19* translation and/or potential transregulation of *IGF2* translation.

Another epigenetic element recently implicated in the control of *IGF2* imprinting is the differentially methylated region (DMR) located upstream of the imprinted *IGF2* promoters. This DMR normally carries a maternal methylation mark in both mouse and human, but this methylation is specifically reduced or lost in Wilms' tumors (28) and colorectal cancers (14-16) and this correlates with *IGF2* LOI (14, 15).

We sought to determine whether *IGF2* LOI or deregulated *H19* expression might explain the elevated levels of *IGF2* transcripts frequently observed in serous epithelial ovarian cancers. We also examined the epigenetic profiles of the *IGF2/H19* domain in these tumors to determine if deregulated methylation status correlated with *IGF2* expression and potential LOI.

Results

Our recent microarray analysis of serous epithelial ovarian cancers indicated that *IGF2* was expressed at high levels in more than half of the cases analyzed compared with normal ovarian surface epithelium. We independently validated the microarray data using quantitative real-time reverse transcription-PCR (1) and these specimens and others were analyzed in the present study. There are several DMRs in the *IGF2/H19* imprinted domain that contribute to regulation of *IGF2* expression and may therefore be involved in the overexpression observed in the ovarian tumors. One of these is located upstream of the imprinted *IGF2* promoters (Fig. 1) and is normally maternally methylated (*IGF2* DMR; ref. 28), whereas another is located upstream of *H19* and is paternally methylated (29). The latter region harbors sequences known to bind to the zinc finger protein CTCF in a methylation-sensitive manner (18, 30). Altered methylation of each of these regions bears relevance to various types of cancer.

IGF2 *DMR*

We first examined the methylation profile of the *IGF2* DMR by PCR and nucleotide sequencing followed by determining the percent methylation for each of the CpG dinucleotides using phosphorimaging analysis. Lymphocytes from individuals without evident malignancy (n = 43) exhibited an average

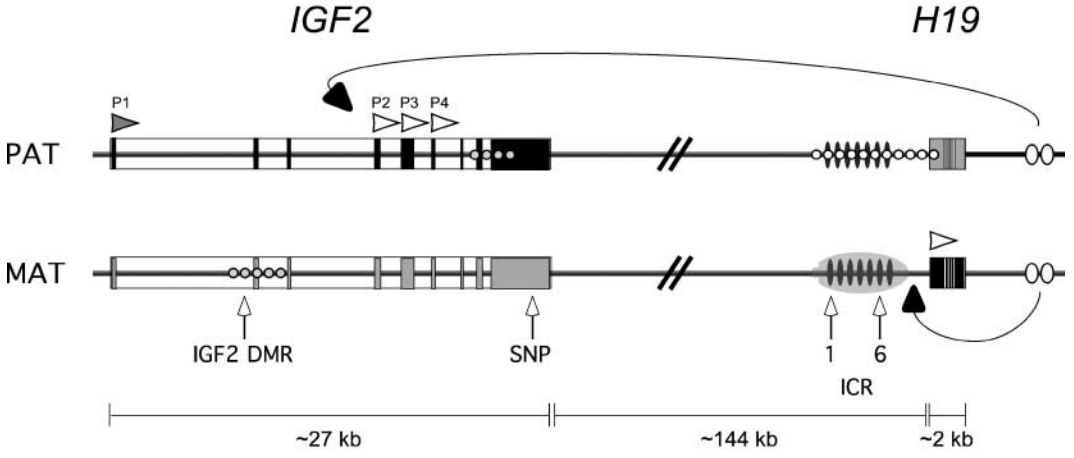

FIGURE 1. Schematic representation of the imprinted *IGF2/H19* domain at 11p15.5 (not to scale). *IGF2* and *H19* are paternally and maternally expressed, respectively, and are separated by ~144 kb of intervening sequence. Vertical bars, exons; black, expressed allele, gray, silenced allele; arrowheads, direction of transcription for *IGF2* and *H19*; white, imprinted expression (*P2, P3*, and *P4* promoters of *IGF2* and *H19* promoter); gray, nonimprinted expression (*IGF2 P1* promoter). There are three known DMRs in the *IGF2/H19* domain; they are indicated by the allele-specific methylation (gray circles). The intergenic sequence contains a differentially methylated imprint control region that harbors seven binding sites (*vertical ovals*) for the zinc finger protein, CTCF (represented as one horizontal oval). Methylation on the paternal chromosome (*PAT*) blocks CTCF binding, silences the *H19* promoter, and allows activation of paternal *IGF2* transcription by downstream enhancers (*white ovals*). Methylation on the maternal chromosome (*MAT*) upstream of the imprinted *IGF2* promoters (*IGF2* DMR) is thought to contribute to maternal *IGF2* silencing. Abnormal maternal activation of *IGF2* can occur through hypomethylation of the *IGF2* DMR and/or hypermethylation of the CTCF-binding sites. CTCF-binding sites 1 and 6 were examined in the present study. Note the relative position of the SNP used to analyze potential *IGF2* LOI in ovarian cancer.

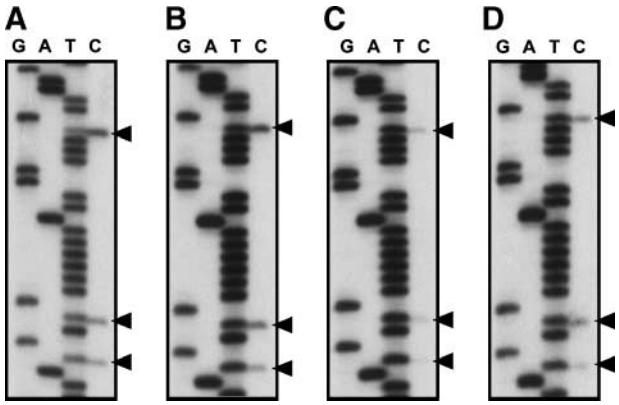

FIGURE 2. *IGF2* DMR methylation. Representative bisulfite sequencing reactions for the *IGF2* DMR showing differential methylation of CpG dinucleotides (*arrowheads*) in normal ovarian surface epithelium (**A**) and in one tumor (**B**) and hypomethylation in two tumors (**C** and **D**).

methylation level of 38.3 ± 9.6% for the *IGF2* DMR (Fig. 2). The methylation status was confirmed for selected samples by sequencing individual cloned alleles following PCR amplification of the bisulfite-treated DNA (data not shown).

Of 72 tumors, 20 exhibited hypomethylation of this DMR (defined as an average methylation level <20% or ~2 SDs below the average level observed in normal lymphocytes), but this did not correlate with the expression of *IGF2* based on the microarray data ($P = 0.15$), with survival ($P = 1.0$), or with age at diagnosis ($P = 0.21$; see Table 1; data with matching microarray values are summarized in Fig. 3). In contrast to the frequent hypomethylation observed in ovarian cancer, only 2 of 43 lymphocyte samples from individuals without malignancy exhibited hypomethylation of this region ($P = 0.004$).

H19 *Expression*

H19 has been implicated previously in the negative regulation of *IGF2* and has been proposed to function as a tumor suppressor (26, 27). We therefore analyzed the expression level of *H19* and compared it with that of *IGF2* to determine if there was any correlation between transcript levels of these genes in serous epithelial ovarian malignancies. We did quantitative real-time reverse transcription-PCR (Taqman) using assays specific for *IGF2* and *H19* with the expression values normalized to those obtained in parallel for *β2-microglobulin* (*B2M*) in a subset of the cancer specimens. Linear regression showed lack of correlation between expression of *IGF2* and *H19* in these tumors ($r^2 = 0.016$; $P = 0.54$; data not shown).

CTCF-Binding Sites at IGF2/H19 *DMR*

We next examined the methylation profile of the imprint control region and specifically focused on two of the seven CTCF-binding sites located within this region that have been shown previously to exhibit methylation abnormalities in other cancers (23). We examined the methylation profile of these two CTCF-binding sites (5′-CCGCGCGGCGGC-3′; ref. 15) using bisulfite sequencing (see Fig. 4A and B for representative data).

Table 1. Epigenetic Analysis of *IGF2* in Serous Epithelial Ovarian Tumors

Characteristic	*n*	Age (Avg)	CTCF-1*	CTCF-6*, †	*IGF2* DMR ‡	LOI§
Borderline	5	41.4	2/2	0/5	2/3	0/2
Early stage (I/II)	9	55.2	6/2	1/8	4/5	0/2
Advanced stage (III/IV)	64	60.9	37/16	28/29	14/44	5/16
Normal lymphocytes‖	43	N/A	3/30	2/37	2/41	N/A
Age at diagnosis (y)						
≤50	17	44.9	10/5	5/11	7/10	1/3
>50	56	64.8	33/13	24/25	11/39	4/15
Fisher's exact *P*			1.00	0.27	0.21	1.00
Survival (advanced stage)						
≤3 y postdiagnosis	30	59.7	16/6	12/13	7/20	3/7
≥7 y postdiagnosis	24	60.1	15/6	11/11	6/15	2/7
Fisher's exact *P*			1.00	1.00	1.00	1.00
***IGF2* expression**						
Microarray ≤90	26	57.6	11/9	5/17	10/14	4/3
Microarray >90	35	60.7	25/5	18/14	7/24	1/12
Fisher's exact *P*			0.05	0.02	0.15	0.03
Epigenetic features						
Borderline vs malignant			0.58¶	0.07¶	0.61¶	1.00¶
Stage I/II vs III/IV			1.00¶	0.07¶	0.24¶	1.00¶
Malignant vs lymphocytes			<0.0001¶	<0.0001¶	0.004¶	N/A

Abbreviation: N/A, not applicable.
*Number exhibiting hypermethylation/number exhibiting differential methylation.
†One sample was not tabulated here because it was hypermethylated at CTCF-6.
‡Number exhibiting hypomethylation/number exhibiting differential methylation.
§Number with loss of *IGF2* imprinting/number with maintenance of imprinting.
‖Normal lymphocytes were from individuals without evident malignancy.
¶Fisher's exact *P*.

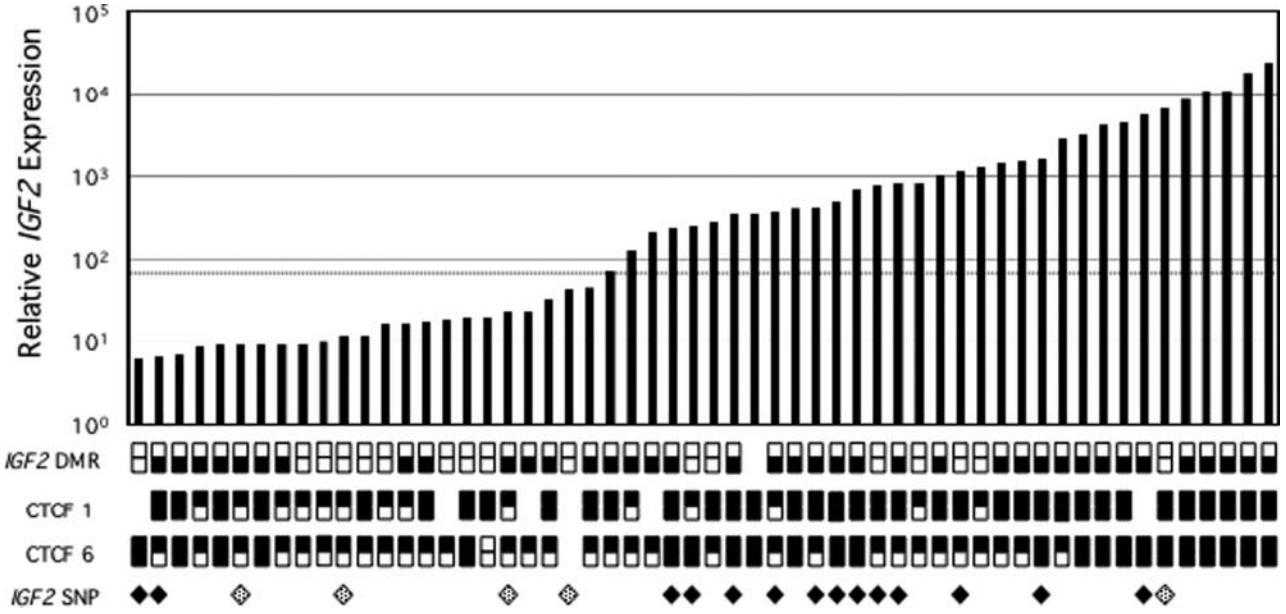

FIGURE 3. Summary of *IGF2* expression and corresponding epigenetic profile. Y axis, relative expression of *IGF2* from 56 serous ovarian tumors detected by hybridization to Affymetrix U133A GeneChip Arrays (Santa Clara, CA; ref. 1). Dominos, methylation status for each tumor sample at the *IGF2* DMR and CTCF sites 1 and 6; filled squares, presence of methylation; half-filled dominos, differential methylation (*top* and *bottom domino halves,* paternal and maternal alleles, respectively). The absence of a domino indicates that the sample was not analyzed. Diamonds, heterozygosity at the *IGF2* SNP used for imprint determination; stippled diamonds, tumors with abnormal activation of maternal *IGF2* (LOI); dashed line, *IGF2* expression averaged for three normal ovarian surface epithelium specimens (average relative expression, 92.8).

For a subset of the cancer cases (n = 8; Fig. 4C) and normal lymphocytes (n = 17; data not shown), the methylation status was also examined using phosphorimaging analysis. We found that CTCF-binding site hypermethylation, defined by an average methylation level of ≥70% for the CpGs contained within the CTCF sites, was much more frequent in advanced-stage disease for both sites combined (~59% of the total sites examined) than borderline (22%) or early-stage (41%) disease (Table 1). In normal lymphocytes, 7% of these sites exhibited hypermethylation. When analyzed independently, CTCF site 1 was more frequently hypermethylated than site 6. Although 39% of the serous tumors were hypermethylated at both CTCF sites, 3% were hypermethylated at site 6 only, whereas 31% were hypermethylated only at site 1. One cancer specimen exhibited hypermethylation of CTCF site 1, whereas CTCF site 6 was hypomethylated (see Figs. 3 and 4C).

To further verify our data for the methylation status of CTCF sites 1 and 6, we cloned PCR amplicons generated from the bisulfite-modified DNA into plasmid vectors where each clone contains a single allele generated from the PCR. We then sequenced multiple individual cloned alleles for each of four tumor specimens (Fig. 4D). Tumor 1 in Fig. 4D exhibits elevated *IGF2* expression, hypermethylation of both CTCF sites 1 and 6 as determined by bisulfite sequencing of the PCR amplicon pool, and *IGF2* LOI. In agreement with our prior assessment, the cloned alleles from both CTCF sites in this tumor are predominantly methylated. This individual is heterozygous for a CpG-altering C/T single nucleotide polymorphism (SNP) in CTCF site 6 (position 7966 of accession no. AF125183) and another nearby A/T SNP (position 8008 of accession no. AF125183). As such, the parental alleles can be distinguished from the sequence. In this case, there was one clone (7966T and 8008A) that was completely unmethylated, suggesting that it may have been derived from normal cells (fibroblasts, stroma, lymphocytes, etc.) present in the tumor tissue used to purify DNA for this sample. Because the maternal allele is normally unmethylated, these results suggest that the 7966T/8008A allele is maternally derived as are the other 7966T/8008A clones that are unmethylated at CpG site 7. The remaining clones are methylated at site 7, are 7966C/8008T, and are therefore likely paternally derived. Similarly, tumor 2 (corresponding to tumor 7 in Fig. 4C) also exhibits very high *IGF2* expression and 89.2%

FIGURE 4. Methylation of CTCF-binding sites 1 and 6. **A** and **B.** Nucleotide sequence of bisulfite-converted DNA across CTCF-binding site 1 (**A**; using forward primer; CTCF site is indicated by the brackets) and site 6 (**B**; using reverse primer) in lymphocytes from healthy individuals showing normal differential methylation (*1-3* in **A** and **B**) and from serous ovarian carcinomas showing normal (*A4*) and hypermethylated CpG dinucleotides (*A5-A7* and *B4-B7*). **B.** Samples 1 and 4 contain a CpG-altering SNP within CTCF-binding site 6. **C.** To validate the CTCF site methylation status observed using radiography, we analyzed eight advanced-stage serous ovarian cancers for the percent methylation of CpGs within the CTCF-binding sites 1 (*dark bars*) and 6 (*light bars*) using phosphorimaging. Note that sample 1 was determined by radiography, phosphorimaging, and by sequencing cloned alleles (see **D**) to exhibit hypermethylation of CTCF site 1 and hypomethylation of CTCF site 6. **D.** Methylation status of individual cloned alleles for four serous ovarian carcinomas at CTCF sites 1 and 6 determined by nucleotide sequencing and shown in the forward direction. Twelve CpG sites were analyzed for each clone; each clone is represented by a row of 12 boxes; each box is an individual CpG dinucleotide (*filled box,* methylated; *unfilled box,* unmethylated). The four CpG dinucleotides within the core CTCF-binding sites 1 and 6 are indicated by shading.

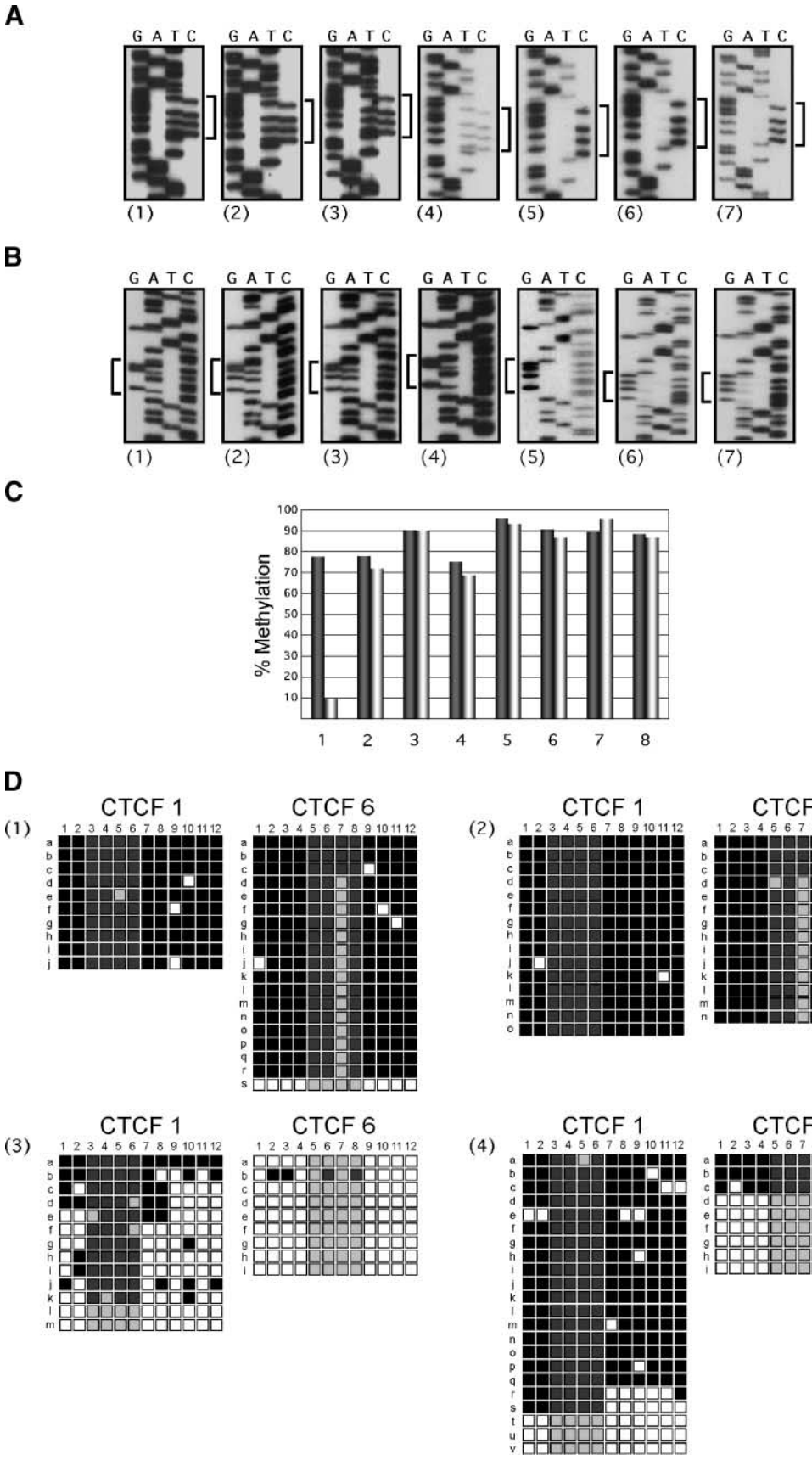
A
G A T C
(1) (2) (3) (4) (5) (6) (7)
B
G A T C
(1) (2) (3) (4) (5) (6) (7)
C
% Methylation
100 90 80 70 60 50 40 30 20 10
1 2 3 4 5 6 7 8
D
(1)
CTCF 1
CTCF 6
(2)
CTCF 1
CTCF 6
(3)
CTCF 1
CTCF 6
(4)
CTCF 1
CTCF 6

methylation at CTCF site 1 and 95.5% methylation at CTCF site 6 (excluding CpG 7 because it is polymorphic in this individual) by phosphorimaging analysis. The results obtained from sequencing cloned alleles from this tumor again agree with the phosphorimaging results, with both CTCF sites exhibiting near complete methylation. This individual is also heterozygous for both SNPs within the sequenced region, but parental identity cannot be determined because all alleles are heavily methylated.

For tumor 3 in Fig. 4D (corresponding to tumor 1 in Fig. 4C) with low *IGF2* expression, the status of the cloned alleles also corroborates our phosphorimaging analysis, where we observed 77.0% and 9.7% methylation of CTCF sites 1 and 6, respectively. Intriguingly, the hypermethylation present within the genomic region encompassing CTCF site 1 seems to specifically target the core CpGs within this binding site. Finally, tumor 4 exhibits elevated *IGF2* expression and was assigned a hypermethylated status for CTCF site 1 and normal differentially methylated status for CTCF site 6 by bisulfite sequencing. Analysis of the cloned alleles completely corroborates the bisulfite sequencing results. Together, these data indicate that there is good correlation between methylation results obtained by bisulfite sequencing, phosphorimaging, and sequencing of cloned alleles for these sites.

We did not find that there were differences in the methylation profile of these sites that correlated with age at diagnosis, survival, or stage of disease. However, cancers with *IGF2* expression levels greater than the average observed for normal ovarian surface epithelium (92.8; $n = 3$) by microarray analysis were significantly more likely to be hypermethylated at CTCF site 1 ($P = 0.05$) or CTCF site 6 ($P = 0.02$) than cancers with low *IGF2* expression (Table 1).

IGF2 Imprinting

To determine if increased *IGF2* expression was associated with *IGF2* LOI, we identified 24 tumors that were heterozygous for a SNP in exon 9 of *IGF2* and compared the nucleotide sequence of their genomic DNA with tumor cDNA (Fig. 5). Of the 24 heterozygotes, 5 exhibited biallelic *IGF2* expression. Surprisingly, 4 of the 5 expressed *IGF2* transcripts in amounts less than that observed in normal ovarian surface epithelium, whereas 1 exhibited high *IGF2* expression. There were no significant associations identified between the tumors that exhibit *IGF2* LOI and either hypomethylation of the *IGF2* DMR ($P = 0.29$) or hypermethylation of the CTCF-binding sites ($P = 0.06$ and 0.60 for sites 1 and 6, respectively).

The specimens used in these analyses were determined to contain >60% malignant cells by a pathologist; nevertheless, we wanted to assess whether the infrequent LOI was due to a potential masking effect from contribution of normal stroma and/or fibroblast cells within the frozen tumor tissues. Sections (5 μm) of the frozen tumors were prepared for several individuals heterozygous for the *IGF2* exon 9 SNP. We then used laser capture microdissection to isolate enriched tumor cell populations for each sample. Reverse transcription-PCR and nucleotide sequencing were done, and in each case, *IGF2* imprinting was maintained even for tumors with 4- and 88-fold increased expression of *IGF2* compared with that observed in normal ovarian surface epithelium (Fig. 5G and H, respectively). We also found maintenance of imprinting where *IGF2* expression was down-regulated relative to that observed in normal ovarian surface epithelium (Fig. 5I).

Discussion

This study is the largest to date that has analyzed the quantitative expression of *IGF2* combined with potential LOI in gynecologic malignancies. It is also the first to begin to examine the epigenetic characteristics of the *IGF2/H19* imprinted domain in ovarian cancers in the context of elevated *IGF2* expression. We have shown that there are substantial changes in the normal methylation profile of specific regions within the *IGF2/H19* imprinted domain, including those associated previously with other types of cancer. We have also determined that ~22% of informative serous epithelial ovarian cancers exhibit *IGF2* LOI but, surprisingly, LOI in these cancers is not correlated with elevated *IGF2* expression levels.

The DMR upstream of the *IGF2* imprinted promoters exhibits substantial hypomethylation in serous epithelial ovarian cancers, but this change is not associated with *IGF2* LOI. This is an unexpected result based on the prior reports of association between hypomethylation of this DMR, LOI, and incidence of colon cancer (14-16). This could be explained by loss of heterozygosity specific to the maternal chromosome, although it is unclear what advantage loss of the normally silent maternal allele would confer to tumor growth unless the locus driving such loss is linked to *IGF2*. Our results from serous ovarian cancers suggest that there is considerable tissue-specific variability in the ability of the *IGF2* DMR to affect imprinting of *IGF2*. We did find hypomethylation of this region in a small fraction of the lymphocyte DNAs we analyzed from women without malignancy, and this observation is consistent with the proportion of the general population reported to have this characteristic (14).

A role for noncoding RNAs is implicated in the regulation of imprinted genes due to the preponderance of these transcribed sequences located in imprinted domains and empirical data suggesting their importance (26, 27, 31-42). For example, the genes *Delta, Drosophila homologue-like 1* (*DLK1*) and *maternally expressed gene 3* (*MEG3*) in the imprinted domain on human chromosome 14 bear remarkable similarity to the *IGF2/H19* domain in terms of the genomic organization and putative regulatory features (43-45). A regulatory role has been postulated for *MEG3* RNA in modulating the expression of the paternally expressed *DLK1*. This is based on analysis of these two genes in sheep (*Ovis aries*) that exhibit a muscular hypertrophy phenotype characterized by enhanced *DLK1* expression and maintenance of normal imprinting (31). In this case, the ratio of expression of the protein coding to the RNA encoding gene seems to be an important factor in the development of the hypertrophic phenotype. It is plausible that a similar regulatory scenario for the *IGF2/H19* domain occurs in ovarian cancer as has been postulated (26, 27). However, we determined the ratio of expression of *H19* mRNA in 26 of these cancers to the level of *IGF2* expression using quantitative real-time reverse transcription-PCR and found no

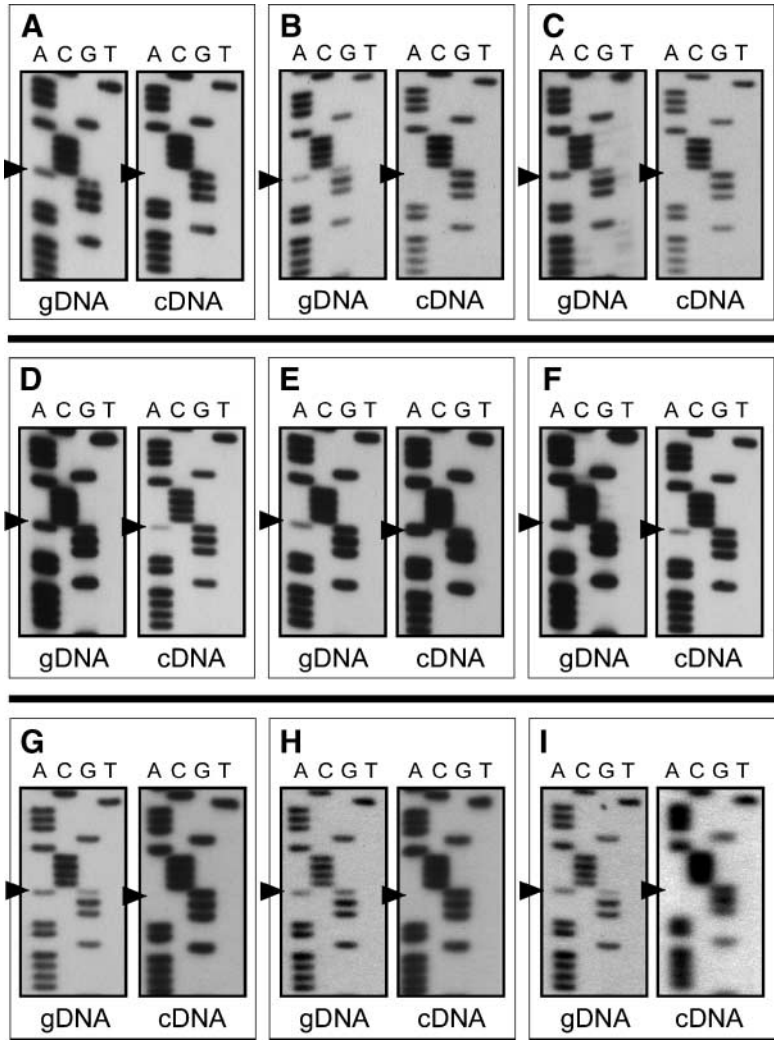

FIGURE 5. *IGF2* imprint analysis. Genomic DNA (*gDNA*) and matched cDNA from advanced-stage serous ovarian tumors of nine individuals for the SNP located in exon 9 of *IGF2* (*arrowheads*). **A** to **C.** Maintenance of *IGF2* imprinting. **D** to **F.** LOI, evidenced by abnormal expression of the maternally inherited *IGF2* allele. **G** to **I.** Maintenance of *IGF2* imprinting. Obtained using RNA isolated from laser capture microdissected tumor cells.

statistical correlation between expression levels of these genes. These results indicate that the level of *H19* RNA produced in serous epithelial ovarian cancers is unlikely to be critical for regulation of *IGF2* expression.

In contrast to the 22% LOI we observed in serous ovarian cancers, LOI in Wilms' tumors can approach 90% for specific subtypes (11), whereas the incidence in colorectal carcinoma is ~44% (46). Previous studies agree with our findings that elevated *IGF2* levels, but relatively infrequent LOI of *IGF2*, are characteristic of serous ovarian adenocarcinomas. Yun et al. reported that although *IGF2* is overexpressed in ovarian cancers, LOI was not an apparent contributing factor in seven informative serous cases (47). Kim et al. also showed that *IGF2* LOI was not a prominent mechanism for *IGF2* overexpression in serous epithelial tumors, but *IGF2* LOI was actually more frequently observed in benign tumors (48).

Although these results indicate that LOI is not a frequent event in ovarian cancers and that LOI does not consistently lead to elevated expression of *IGF2* in serous epithelial tumors, they do not account for the elevated expression of *IGF2* observed in about half of the cases we analyzed. Overexpression of *IGF2* is clinically relevant and it is therefore important to understand how this occurs in serous epithelial ovarian cancer in the absence of LOI. Our results now implicate an imprinting-independent role for hypermethylation at the *IGF2* imprint control region in the overexpression of *IGF2*. Current dogma holds that hypermethylation of the CTCF sites within the imprint control region blocks CTCF binding, leading to *IGF2* LOI (Fig. 1). This is the first report to our knowledge that links aberrant hypermethylation of this imprint control region to elevated *IGF2* expression with maintenance of normal imprinting and again underscores the complexity associated with the transcriptional regulation of this domain.

Our data suggest that whereas the maternal *IGF2* allele remains silent the paternal allele in many tumors has become more transcriptionally proficient. It is unclear how biallelic CTCF site methylation would contribute to enhanced *IGF2* expression from only the paternal allele. This could be due to changes in histone acetylation or histone methylation status (e.g., see refs. 49, 50) that promote increased *IGF2* expression

from the paternal allele, more efficient transcriptional activation via transcription factor binding to the paternal allele, or other epigenetic changes that regulate *IGF2* expression. In this regard, analysis of the methylation status of the intragenic DMR of *IGF2* (see Fig. 1) would help determine whether this region, which was shown previously to be evolutionarily conserved among imprinted mammals and to contain putative CTCF-binding sites (51), is epigenetically modulating *IGF2* expression in ovarian cancer.

The high frequency of epigenetic alterations observed in serous epithelial ovarian cancers at the *IGF2/H19* domain suggests that these changes may serve as a useful disease biomarker. Of the three epigenetic markers we analyzed, only 13% of the specimens exhibited a normal methylation profile. Of particular relevance, each cancer in this study that was diagnosed at an early stage (I/II; $n = 9$) exhibited *IGF2* DMR hypomethylation and/or CTCF site 1 hypermethylation. In contrast, hypermethylation of CTCF site 6 was found mostly in advanced cases. Unlike CTCF site 1 hypermethylation, *IGF2* DMR hypomethylation was not associated with high expression of *IGF2*. Nevertheless, both epigenetic changes may be an early indicator of disease. One of the major limitations to the successful treatment of women with epithelial ovarian cancer is the difficulty in detecting early-stage disease. Additional studies are required to evaluate the potential to use epigenetic characteristics, like those reported here for the *IGF2/H19* domain, to improve the ability to detect early-stage disease by analyzing tumor DNA present in serum, plasma, or peritoneal fluid. Further evaluation of the mechanistic basis for epigenetic-mediated up-regulation of *IGF2* could also lead to development of novel therapeutic targets.

Materials and Methods

Samples

Borderline (low malignant potential), early-stage (I or II), and advanced-stage (III or IV) serous ovarian carcinomas (see Table 1), normal ovarian tissues, and peripheral blood lymphocytes (from individuals without evident malignancy) were obtained and used with approval from the Institutional Review Board of Duke University. Samples were immediately processed and stored at −80°C before nucleic acid extraction. DNA was prepared using standard phenol/chloroform extraction followed by ethanol precipitation. RNA was prepared using the Qiagen RNeasy Mini kit (Valencia, CA).

Methylation Analyses

Genomic DNA (1 μg) was treated with sodium bisulfite as described previously (52, 53). Sodium bisulfite converts unmethylated cytosines to uracils, whereas methylated cytosines are unaffected. Bisulfite-treated DNA (20-50 ng) was subsequently used as template in PCR. Primers were designed to amplify the bisulfite-converted DNA by annealing to regions devoid of CpG dinucleotides to avoid bias in amplification. Primer sequences (5′-3′) include *IGF2* DMR TAATTTATTTAGGGTGGTGTT (forward) and TCCAAACACCCCCACCTTAA (reverse; ref. 15), CTCF site 1 GTATAGGTATTTTTGGAGGTTTTTTA (forward) and CCTAAAATAAATCAAACACATAACCC (reverse; ref. 23), and CTCF site 6 GTATATGGGTATTTTTGGAGGT (forward) and CTTAAATCCCAAACCATAACACTA (reverse; ref. 15). PCR amplicons were resolved on agarose gels and purified using Sigma GenElute spin columns (St. Louis, MO) or directly using the Qiagen MinElute PCR Purification kit. The amplicons were manually sequenced with the Thermosequenase Dideoxy Terminator Cycle Sequencing kit (U.S. Biologicals, Swampscott, MA) using the following primers: *IGF2* DMR (forward primer listed above), CTCF site 1 (GAGGTTTTTTATTTTAGTTTTGG), and CTCF site 6 (TATCCTATTCCCAAATAACC). Following resolution of the sequencing reactions on denaturing polyacrylamide gels, the gel was exposed to radiographic film (Kodak X-OMAT MR, New Haven, CT) and/or a phosphorimager screen followed by percent methylation determination using the Storm PhosphorImager System and ImageQuant Software (GE Healthcare Life Sciences, Piscataway, NJ). Specimens with average methylation of <20% for the three CpGs in the *IGF2* DMR were considered to exhibit hypomethylation, whereas those exhibiting methylation levels ≥70% for the CpGs within CTCF sites 1 and 6 were considered hypermethylated.

For analysis of the methylation status of individual alleles, PCR amplicons were generated as described above and resolved on 2% agarose gels. Following purification with the Qiagen MinElute PCR Cleanup kit, the amplicons were ligated into pGEMT-Easy vectors (Promega, Madison, WI) and plasmids were transformed into competent JM109 *Escherichia coli* (Promega) followed by plating to LB agar with 100 μg/mL ampicillin (Teknova, Hollister, CA). Whole-cell PCR was used to amplify plasmids from individual colonies using SP6 and T7 primers (94°C for 5 minutes followed by 35 cycles of 94°C for 30 seconds, 55°C for 30 seconds, and 72°C for 30 seconds and a final 5-minute extension at 72°C). The amplicons were resolved on agarose gels, purified using Sigma GenElute spin columns, and sequenced.

Quantitative Real-time Reverse Transcription-PCR

Total RNA (1 μg) was reverse transcribed in a 20 μL reaction volume with random hexamer primers using the AMV First-Strand cDNA Synthesis kit (Roche, Basel, Switzerland). Subsequent real-time PCRs (Taqman Assays-On-Demand; *IGF2*, Hs00171254_m1; *H19*, Hs00399294_g1; Applied Biosystems, Foster City, CA) were done using 11.25 μL of a 1:15 dilution of the cDNA according to the manufacturer's recommendations on an ABI Prism 7900HT Sequence Detection System (Applied Biosystems) with the exception that a 25 μL reaction volume was used with 50 total cycles. The relative expression levels of *IGF2* and *H19* were obtained for each sample by normalization to the expression level of *B2M* (Taqman Assays-on-Demand, Hs99999907_m1). All assays were done in parallel.

Imprint Status Determination

DNA from tumors was genotyped for a SNP located in exon 9 of *IGF2* using primers CTTGGACTTTGAGTCAAATTGG (forward) and GGTCGTGCCAATTACATTTCA (reverse). cDNAs generated from DNase I–treated RNAs of heterozygotes were analyzed for allelic expression by manual

nucleotide sequencing with the forward primer. Laser capture microdissection using an Arcturus PixCell II LCM System (Mountain View, CA) was done on selected tumors to isolate homogeneous populations of tumor cells to confirm imprint status. Samples with evident biallelic cDNA expression were considered to exhibit LOI.

Statistical Analysis

Fisher's exact tests were used to calculate two-sided *P*s using InStat 3.0 for Mac (GraphPad Software, San Diego, CA) to determine if there were nonrandom associations between categorical variables. *P*s $\leq$ 0.05 were considered significant.

Acknowledgments

We thank Jennifer Clarke for assistance with statistical analysis.

References

1. Berchuck A, Iversen ES, Lancaster JM, et al. Patterns of gene expression that characterize long-term survival in advanced stage serous ovarian cancers. Clin Cancer Res 2005;11:3686–96.

2. Sayer RA, Lancaster JM, Pittman J, et al. High insulin-like growth factor-2 (*IGF2*) gene expression is an independent predictor of poor survival for patients with advanced stage serous epithelial ovarian cancer. Gynecol Oncol 2005;96: 355–61.

3. Mor G, Visintin I, Lai Y, et al. Serum protein markers for early detection of ovarian cancer. Proc Natl Acad Sci U S A 2005;102:7677–82.

4. Reik W, Constancia M, Dean W, et al. *Igf2* imprinting in development and disease. Int J Dev Biol 2000;44:145–50.

5. Foulstone E, Prince S, Zaccheo O, et al. Insulin-like growth factor ligands, receptors, and binding proteins in cancer. J Pathol 2005;205:145–53.

6. Pollak M. The question of a link between insulin-like growth factor physiology and neoplasia. Growth Horm IGF Res 2000;10 Suppl B:S21–4.

7. Ulaner GA, Vu TH, Li T, et al. Loss of imprinting of *IGF2* and *H19* in osteosarcoma is accompanied by reciprocal methylation changes of a CTCF-binding site. Hum Mol Genet 2003;12:535–49.

8. Kohda M, Hoshiya H, Katoh M, et al. Frequent loss of imprinting of *IGF2* and *MEST* in lung adenocarcinoma. Mol Carcinog 2001;31:184–91.

9. el-Naggar AK, Lai S, Tucker SA, et al. Frequent loss of imprinting at the *IGF2* and *H19* genes in head and neck squamous carcinoma. Oncogene 1999; 18:7063–9.

10. Rainho CA, Kowalski LP, Rogatto SR. Loss of imprinting and loss of heterozygosity on 11p15.5 in head and neck squamous cell carcinomas. Head Neck 2001;23:851–9.

11. Ravenel JD, Broman KW, Perlman EJ, et al. Loss of imprinting of insulin-like growth factor-II (*IGF2*) gene in distinguishing specific biologic subtypes of Wilms tumor. J Natl Cancer Inst 2001;93:1698–703.

12. Jarrard DF, Bussemakers MJ, Bova GS, Isaacs WB. Regional loss of imprinting of the insulin-like growth factor II gene occurs in human prostate tissues. Clin Cancer Res 1995;1:1471–8.

13. Takano Y, Shiota G, Kawasaki H. Analysis of genomic imprinting of insulin-like growth factor 2 in colorectal cancer. Oncology 2000;59:210–6.

14. Cui H, Cruz-Correa M, Giardiello FM, et al. Loss of *IGF2* imprinting: a potential marker of colorectal cancer risk. Science 2003;299:1753–5.

15. Cui H, Onyango P, Brandenburg S, Wu Y, Hsieh CL, Feinberg AP. Loss of imprinting in colorectal cancer linked to hypomethylation of *H19* and *IGF2*. Cancer Res 2002;62:6442–6.

16. Cruz-Correa M, Cui H, Giardiello FM, et al. Loss of imprinting of insulin growth factor II gene: a potential heritable biomarker for colon neoplasia predisposition. Gastroenterology 2004;126:964–70.

17. Nakagawa H, Chadwick RB, Peltomaki P, Plass C, Nakamura Y, de La Chapelle A. Loss of imprinting of the insulin-like growth factor II gene occurs by biallelic methylation in a core region of *H19*-associated CTCF-binding sites in colorectal cancer. Proc Natl Acad Sci U S A 2001;98: 591–6.

18. Wolffe AP. Transcriptional control: imprinting insulation. Curr Biol 2000;10: R463–5.

19. Davis TL, Yang GJ, McCarrey JR, Bartolomei MS. The *H19* methylation imprint is erased and re-established differentially on the parental alleles during male germ cell development. Hum Mol Genet 2000;9:2885–94.

20. Klenova EM, Morse HC III, Ohlsson R, Lobanenkov VV. The novel BORIS + CTCF gene family is uniquely involved in the epigenetics of normal biology and cancer. Semin Cancer Biol 2002;12:399–414.

21. Ohlsson R, Renkawitz R, Lobanenkov V. CTCF is a uniquely versatile transcription regulator linked to epigenetics and disease. Trends Genet 2001;17: 520–7.

22. Takai D, Gonzales FA, Tsai YC, Thayer MJ, Jones PA. Large scale mapping of methylcytosines in CTCF-binding sites in the human *H19* promoter and aberrant hypomethylation in human bladder cancer. Hum Mol Genet 2001;10: 2619–26.

23. Cui H, Niemitz EL, Ravenel JD, et al. Loss of imprinting of insulin-like growth factor-II in Wilms' tumor commonly involves altered methylation but not mutations of CTCF or its binding site. Cancer Res 2001;61:4947–50.

24. Moulton T, Crenshaw T, Hao Y, et al. Epigenetic lesions at the *H19* locus in Wilms' tumour patients. Nat Genet 1994;7:440–7.

25. Steenman MJ, Rainier S, Dobry CJ, Grundy P, Horon IL, Feinberg AP. Loss of imprinting of *IGF2* is linked to reduced expression and abnormal methylation of *H19* in Wilms' tumour. Nat Genet 1994;7:433–9.

26. Wilkin F, Paquette J, Ledru E, et al. *H19* sense and antisense transgenes modify insulin-like growth factor-II mRNA levels. Eur J Biochem 2000;267: 4020–7.

27. Li YM, Franklin G, Cui HM, et al. The *H19* transcript is associated with polysomes and may regulate *IGF2* expression in trans. J Biol Chem 1998;273: 28247–52.

28. Sullivan MJ, Taniguchi T, Jhee A, Kerr N, Reeve AE. Relaxation of *IGF2* imprinting in Wilms tumours associated with specific changes in *IGF2* methylation. Oncogene 1999;18:7527–34.

29. Jinno Y, Sengoku K, Nakao M, et al. Mouse/human sequence divergence in a region with a paternal-specific methylation imprint at the human *H19* locus. Hum Mol Genet 1996;5:1155–61.

30. Robertson KD. DNA methylation and human disease. Nat Rev Genet 2005;6: 597–610.

31. Murphy SK, Freking BA, Smith TJ, et al. Abnormal postnatal maintenance of elevated *DLK1* transcript levels in callipyge sheep. Mamm Genome 2005;16: 171–83.

32. Rougeulle C, Cardoso C, Fontes M, Colleaux L, Lalande M. An imprinted antisense RNA overlaps *UBE3A* and a second maternally expressed transcript. Nat Genet 1998;19:15–6.

33. Nakabayashi K, Bentley L, Hitchins MP, et al. Identification and characterization of an imprinted antisense RNA (*MESTIT1*) in the human *MEST* locus on chromosome 7q32. Hum Mol Genet 2002;11:1743–56.

34. Mitsuya K, Meguro M, Lee MP, et al. *LIT1,* an imprinted antisense RNA in the human *KvLQT1* locus identified by screening for differentially expressed transcripts using monochromosomal hybrids. Hum Mol Genet 1999; 8:1209–17.

35. Runte M, Huttenhofer A, Gross S, Kiefmann M, Horsthemke B, Buiting K. The IC-*SNURF-SNRPN* transcript serves as a host for multiple small nucleolar RNA species and as an antisense RNA for *UBE3A*. Hum Mol Genet 2001;10: 2687–700.

36. Sleutels F, Zwart R, Barlow DP. The non-coding Air RNA is required for silencing autosomal imprinted genes. Nature 2002;415:810–3.

37. Li T, Vu TH, Lee KO, et al. An imprinted *PEG1/MEST* antisense expressed predominantly in human testis and in mature spermatozoa. J Biol Chem 2002; 277:13518–27.

38. Cavaille J, Seitz H, Paulsen M, Ferguson-Smith AC, Bachellerie JP. Identification of tandemly-repeated C/D snoRNA genes at the imprinted human 14q32 domain reminiscent of those at the Prader-Willi/Angelman syndrome region. Hum Mol Genet 2002;11:1527–38.

39. Seitz H, Youngson N, Lin SP, et al. Imprinted microRNA genes transcribed antisense to a reciprocally imprinted retrotransposon-like gene. Nat Genet 2003;34:261–2.

40. de Los Santos T, Schweizer J, Rees CA, Francke U. Small evolutionarily conserved RNA, resembling C/D box small nucleolar RNA, is transcribed from *PWCR1,* a novel imprinted gene in the Prader-Willi deletion region, which is highly expressed in brain. Am J Hum Genet 2000;67:1067–82.

41. Shimoda M, Morita S, Obata Y, Sotomaru Y, Kono T, Hatada I. Imprinting of a small nucleolar RNA gene on mouse chromosome 12. Genomics 2002;79: 483–6.

42. Bidwell CA, Kramer LN, Perkins AC, Hadfield TS, Moody DE, Cockett NE.

Expression of *PEG11* and *PEG11AS* transcripts in normal and callipyge sheep. BMC Biol 2004;2:17.

43. Takada S, Paulsen M, Tevendale M, et al. Epigenetic analysis of the *Dlk1-Gtl2* imprinted domain on mouse chromosome 12: implications for imprinting control from comparison with *Igf2-H19*. Hum Mol Genet 2002;11:77–86.

44. Paulsen M, Takada S, Youngson NA, et al. Comparative sequence analysis of the imprinted *Dlk1-Gtl2* locus in three mammalian species reveals highly conserved genomic elements and refines comparison with the *Igf2-H19* region. Genome Res 2001;11:2085–94.

45. Wylie AA, Murphy SK, Orton TC, Jirtle RL. Novel imprinted *DLK1/GTL2* domain on human chromosome 14 contains motifs that mimic those implicated in *IGF2/H19* regulation. Genome Res 2000;10:1711–8.

46. Cui H, Horon IL, Ohlsson R, Hamilton SR, Feinberg AP. Loss of imprinting in normal tissue of colorectal cancer patients with microsatellite instability. Nat Med 1998;4:1276–80.

47. Yun K, Fukumoto M, Jinno Y. Monoallelic expression of the insulin-like growth factor-2 gene in ovarian cancer. Am J Pathol 1996;148:1081–7.

48. Kim HT, Choi BH, Niikawa N, Lee TS, Chang SI. Frequent loss of imprinting of the *H19* and *IGF-II* genes in ovarian tumors. Am J Med Genet 1998; 80:391–5.

49. Ulaner GA, Yang Y, Hu JF, Li T, Vu TH, Hoffman AR. CTCF binding at the insulin-like growth factor-II (*IGF2*)/*H19* imprinting control region is insufficient to regulate *IGF2/H19* expression in human tissues. Endocrinology 2003;144: 4420–6.

50. Yang Y, Hu JF, Ulaner GA, et al. Epigenetic regulation of *Igf2/H19* imprinting at CTCF insulator binding sites. J Cell Biochem 2003;90: 1038–55.

51. Weidman JR, Murphy SK, Nolan CM, Dietrich FS, Jirtle RL. Phylogenetic footprint analysis of *IGF2* in extant mammals. Genome Res 2004;14:1726–32.

52. Grunau C, Clark SJ, Rosenthal A. Bisulfite genomic sequencing: systematic investigation of critical experimental parameters. Nucleic Acids Res 2001;29: E65–5.

53. Murphy SK, Wylie AA, Coveler KJ, et al. Epigenetic detection of human chromosome 14 uniparental disomy. Hum Mutat 2003;22:92–7.